

On the Angular Momentum Conservation and Incremental Objectivity Properties of a Predictor/Multi-corrector Method for Lagrangian Shock Hydrodynamics [☆]

E. Love^a, G. Scovazzi^{a,*}

^a1431 Computational Shock- and Multi-physics Department, Sandia National Laboratories,
P.O. Box 5800, MS 1319, Albuquerque, NM 87185-1319, USA

Abstract

This article presents an analysis of the global angular momentum conservation and objectivity properties for a predictor/multi-corrector scheme often used in shock hydrodynamics computations in combination with staggered spatial discretizations. As the number of iterations increases, the numerical solution of the predictor/multi-corrector algorithm converges to that of an implicit mid-point time integrator, which preserves global angular momentum and incremental objectivity. In the case of a finite number of iterations, the order of accuracy with which these quantities are preserved is always higher than the order of accuracy of the method, and decays as Δt^{2i} , where i is the iteration index.

Key words: Angular momentum conservation, incremental objectivity, predictor/multi-corrector algorithm, mid-point time integrator, Lagrangian shock hydrodynamics, staggered formulation.

1. Introduction

This article presents an analysis of global angular momentum conservation and incremental objectivity properties for the time-integration algorithm proposed in [7, 8]. This method identically corresponds to the staggered (in space) finite difference formulations of [1, 2] in the case of one spatial dimension, and maintains their structure and many of their properties in multiple dimensions. Based on a predictor/multi-corrector variant of the implicit mid-point time integrator, this approach does not require staggering in time between kinematic and thermodynamic variables to achieve second-order accuracy and ensure conservation of global mass, linear momentum and total energy. The analysis documented in this article also applies to a variation of the algorithm, which uses piecewise linear thermodynamic variables [9].

A number of remarks on angular momentum conservation and incremental objectivity were made in [7, 8] about the time-integrator under discussion, but complete and detailed derivations were missing. This brief article documents the simple derivations to evaluate these results, and was spurred by conversations with members of the research community in shock hydrodynamics, whose comments and observations are thankfully acknowledged.

It is shown that, for an increasing number of iterations, the limit mid-point algorithm preserves global angular momentum

and incremental objectivity. In the case of a finite number of iterations, the order of accuracy with which these quantities are preserved is always higher than the order of accuracy of the method, and decays as a Δt^{2i} , where i is the iteration index.

2. The Lagrangian hydrodynamics system

In order to begin the discussion, we briefly summarize the system of Lagrangian equations for a compressible fluid in which heat fluxes, heat sources, and body forces are absent. Let Ω_0 and Ω be open sets in \mathbb{R}^{n_d} (where n_d is the number of spatial dimensions). The *deformation*

$$\varphi : \Omega_0 \rightarrow \Omega = \varphi(\Omega_0), \quad (1)$$

$$X \mapsto \mathbf{x} = \varphi(X, t), \quad \forall X \in \Omega_0, t \geq 0, \quad (2)$$

maps the material coordinate X , representing the initial position of an infinitesimal material particle of the body, to \mathbf{x} , the position of that particle in the current configuration (see Fig. 1). Ω_0 is the domain occupied by the body in its initial configuration, with boundary Γ_0 . φ maps Ω_0 to Ω , the domain occupied by the body in its current configuration. The *deformation gradient* and *deformation Jacobian determinant* can be defined as

$$\mathbf{F} = \nabla_X \varphi, \quad (3)$$

$$J = \det(\mathbf{F}), \quad (4)$$

where ∇_X is the gradient in the original configuration. In the domain Ω , the equations for the displacement update and con-

[☆]This research was partially funded by the DOE NNSA Advanced Scientific Computing Program and the Computer Science Research Institute at Sandia National Laboratories. Sandia is a multiprogram laboratory operated by Sandia Corporation, a Lockheed Martin Company, for the United States Department of Energy under contract DEAC04-94-AL85000.

*Corresponding author

Email addresses: gscovaz@sandia.gov (G. Scovazzi)

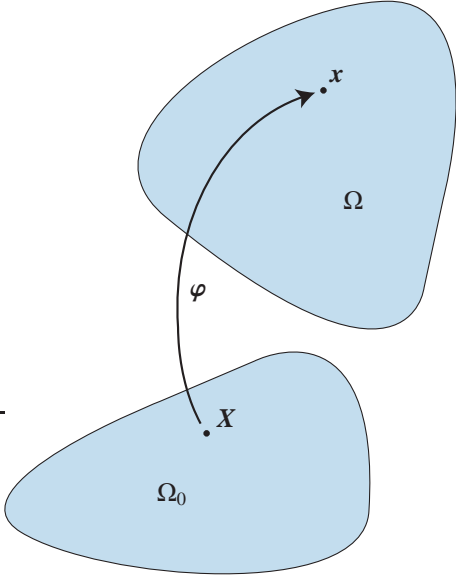


Figure 1: Sketch of the Lagrangian map φ .

servation of mass, momentum, and energy read:

$$\dot{\mathbf{u}} = \mathbf{v} , \quad (5)$$

$$\rho J = \rho_0 , \quad (6)$$

$$0 = \rho \dot{\mathbf{v}} - \nabla_x \cdot \boldsymbol{\sigma} , \quad (7)$$

$$0 = \rho \dot{\epsilon} - \boldsymbol{\sigma} : \nabla_x \mathbf{v} . \quad (8)$$

Here, ∇_x and $\nabla_x \cdot$ are the current configuration gradient and divergence operators, and $(\dot{\cdot})$ indicates the material, or Lagrangian, time derivative. $\mathbf{u} = \mathbf{x} - \mathbf{X}$ is the displacement vector, ρ_0 is the reference (initial) density, ρ is the (current) density, \mathbf{v} is the velocity, $\boldsymbol{\sigma}$ is the Cauchy stress, and ϵ the internal energy per unit mass. In the case of compressible fluids, $\boldsymbol{\sigma} = -p\mathbf{I}$, where p is the thermodynamic pressure, related to density and internal energy by an equation of state of the type $p = \hat{p}(\rho, \epsilon)$.

3. Angular momentum

Following the derivations in [7, 8] or [9] a predictor/multi-corrector algorithm can be designed to integrate the equations of motion in Lagrangian coordinates. The analysis that follows is focused on the conservation of angular momentum, a property which is derived from the equations governing the evolution of linear momentum and displacements. We avoid presenting the discrete form of all other equations, as they are not relevant in the discussion that follows. The Lagrangian weak form of the momentum conservation equation for the predictor/multi-corrector algorithm in [8] reads

$$0 = \int_{\Omega_0} \delta \boldsymbol{\varphi} \cdot \rho_0 (\mathbf{v}_{n+1}^{(i+1)} - \mathbf{v}_n) + \Delta t \int_{\Omega_{n+1/2}^{(i)}} (\nabla_x (\delta \boldsymbol{\varphi}))_{n+1/2}^{(i)} : \boldsymbol{\sigma}_{n+1/2}^{(i)} , \quad (9)$$

where $\delta \boldsymbol{\varphi}$ is an admissible variation of the motion (or, deformation) $\boldsymbol{\varphi}$, n is the time step index, (i) is iterate index, and

the subscript $n + 1/2$ refers to quantities computed at time $t_{n+1/2} = (t_n + t_{n+1})/2$. For the derivations that follow, it is important to notice that the algorithmic Cauchy stress $\boldsymbol{\sigma}$ may contain stabilization and discontinuity capturing terms, in addition to the constitutive stress relationship. The specific form of $\boldsymbol{\sigma}$ is not relevant as long as it is a symmetric tensor, as is the case in [8, 9]. The algorithm is implemented by first computing the new iterate $(i + 1)$ of the velocity at time t_{n+1} and by subsequently updating the position iterate, $\boldsymbol{\varphi}_{n+1}^{(i+1)}$, using

$$\mathbf{0} = \boldsymbol{\varphi}_{n+1}^{(i+1)} - \boldsymbol{\varphi}_n - \Delta t \cdot \mathbf{v}_{n+1/2}^{(i+1)} . \quad (10)$$

To ensure second-order accuracy this iteration must be repeated at least two times. By defining the second Piola symmetric stress tensor \mathbf{S} with the relation

$$\mathbf{J}_{n+1/2}^{(i)} \boldsymbol{\sigma}_{n+1/2}^{(i)} = \mathbf{F}_{n+1/2}^{(i)} \mathbf{S}_{n+1/2}^{(i)} \mathbf{F}_{n+1/2}^{(i)T} , \quad (11)$$

and replacing the algorithmic Cauchy stress $\boldsymbol{\sigma}$ using (11), it is possible to rewrite (9) as

$$0 = \int_{\Omega_0} \delta \boldsymbol{\varphi} \cdot \rho_0 (\mathbf{v}_{n+1}^{(i+1)} - \mathbf{v}_n) + \Delta t \int_{\Omega_0} \nabla_x (\delta \boldsymbol{\varphi}) : (\mathbf{F}_{n+1/2}^{(i)} \mathbf{S}_{n+1/2}^{(i)}) , \quad (12)$$

Considering homogeneous Neumann (zero traction) boundary conditions, an admissible choice for $\delta \boldsymbol{\varphi}$ is $\delta \boldsymbol{\varphi} = \boldsymbol{\xi} \times \boldsymbol{\varphi}_{n+1/2}^{(j)}$, for some $\boldsymbol{\xi} \in \mathbb{R}^3$. This yields

$$\begin{aligned} 0 &= \int_{\Omega_0} \boldsymbol{\xi} \times \boldsymbol{\varphi}_{n+1/2}^{(j)} \cdot \rho_0 (\mathbf{v}_{n+1}^{(i+1)} - \mathbf{v}_n) \\ &\quad + \Delta t \int_{\Omega_0} \nabla_x (\boldsymbol{\xi} \times \boldsymbol{\varphi}_{n+1/2}^{(j)}) : (\mathbf{F}_{n+1/2}^{(i)} \mathbf{S}_{n+1/2}^{(i)}) \\ &= \int_{\Omega_0} \boldsymbol{\xi} \times \boldsymbol{\varphi}_{n+1/2}^{(j)} \cdot \rho_0 (\mathbf{v}_{n+1}^{(i+1)} - \mathbf{v}_n) \\ &\quad + \Delta t \int_{\Omega_0} (\hat{\boldsymbol{\xi}} \mathbf{F}_{n+1/2}^{(j)}) : (\mathbf{F}_{n+1/2}^{(i)} \mathbf{S}_{n+1/2}^{(i)}) \\ &= \int_{\Omega_0} \boldsymbol{\xi} \times \boldsymbol{\varphi}_{n+1/2}^{(j)} \cdot \rho_0 (\mathbf{v}_{n+1}^{(i+1)} - \mathbf{v}_n) \\ &\quad + \Delta t \int_{\Omega_0} \hat{\boldsymbol{\xi}} : (\mathbf{F}_{n+1/2}^{(i)} \mathbf{S}_{n+1/2}^{(i)} \mathbf{F}_{n+1/2}^{(j)T}) \\ &= \boldsymbol{\xi} \cdot \int_{\Omega_0} \boldsymbol{\varphi}_{n+1/2}^{(j)} \times \rho_0 (\mathbf{v}_{n+1}^{(i+1)} - \mathbf{v}_n) \\ &\quad + \Delta t \hat{\boldsymbol{\xi}} : \left(\int_{\Omega_0} \mathbf{F}_{n+1/2}^{(i)} \mathbf{S}_{n+1/2}^{(i)} \mathbf{F}_{n+1/2}^{(j)T} \right) , \end{aligned} \quad (13)$$

where $\hat{\boldsymbol{\xi}}$ is the skew-symmetric tensor satisfying $\hat{\boldsymbol{\xi}} \mathbf{a} = (\boldsymbol{\xi} \times \mathbf{a})$, $\forall \mathbf{a} \in \mathbb{R}^3$. Note that the term

$$\int_{\Omega_0} \boldsymbol{\varphi}_{n+1/2}^{(j)} \times \rho_0 (\mathbf{v}_{n+1}^{(i+1)} - \mathbf{v}_n) \quad (14)$$

represents an algorithmic increment in total angular momentum between time step n and the $(i + 1)$ th iterate at time step $n + 1$, computed using the deformation at the midpoint in time and iterate (j) .

3.1. A limit case: Mid-point integrator

First consider the limit $j, i \rightarrow \infty$, for which we obtain the classical, implicit mid-point integrator. In this case (see also [11]),

$$0 = \boldsymbol{\xi} \cdot \left(\int_{\Omega_0} \boldsymbol{\varphi}_{n+1/2}^{(\infty)} \times \rho_0 (\mathbf{v}_{n+1}^{(\infty)} - \mathbf{v}_n) \right) + \Delta t \hat{\boldsymbol{\xi}} : \left(\int_{\Omega_0} \mathbf{F}_{n+1/2}^{(\infty)} \mathbf{S}_{n+1/2}^{(\infty)} \mathbf{F}_{n+1/2}^{(\infty)T} \right). \quad (15)$$

Removing the superscript (∞) for convenience, using (10) and (11), and defining

$$\Pi_n := \int_{\Omega_n} \boldsymbol{\varphi}_n \times (\rho_n \mathbf{v}_n) = \int_{\Omega_0} \boldsymbol{\varphi}_n \times (\rho_0 \mathbf{v}_n), \quad (16)$$

we can further manipulate (15) into

$$\begin{aligned} 0 &= \boldsymbol{\xi} \cdot \left(\int_{\Omega_0} \left(\boldsymbol{\varphi}_n + \frac{\Delta t}{2} \mathbf{v}_{n+1/2} \right) \times \rho_0 (\mathbf{v}_{n+1} - \mathbf{v}_n) \right) \\ &\quad + \Delta t \hat{\boldsymbol{\xi}} : \left(\int_{\Omega_0} \mathbf{J}_{n+1/2} \boldsymbol{\sigma}_{n+1/2} \right) \\ &= \boldsymbol{\xi} \cdot \left(\int_{\Omega_0} \left(\left(\boldsymbol{\varphi}_n + \frac{\Delta t}{2} \mathbf{v}_{n+1/2} \right) \times (\rho_0 \mathbf{v}_{n+1}) \right) - \Pi_n \right) \\ &\quad - \frac{\Delta t}{2} \boldsymbol{\xi} \cdot \left(\int_{\Omega_0} \mathbf{v}_{n+1/2} \times (\rho_0 \mathbf{v}_n) \right) \\ &= \boldsymbol{\xi} \cdot \left(\int_{\Omega_0} \left(\left(\boldsymbol{\varphi}_{n+1} - \frac{\Delta t}{2} \mathbf{v}_{n+1/2} \right) \times (\rho_0 \mathbf{v}_{n+1}) \right) - \Pi_n \right) \\ &\quad - \frac{\Delta t}{2} \boldsymbol{\xi} \cdot \left(\int_{\Omega_0} \mathbf{v}_{n+1/2} \times (\rho_0 \mathbf{v}_n) \right) \\ &= \boldsymbol{\xi} \cdot \left(\Pi_{n+1} - \Pi_n - \frac{\Delta t}{2} \int_{\Omega_0} \rho_0 \mathbf{v}_{n+1/2} \times (\mathbf{v}_n + \mathbf{v}_{n+1}) \right) \\ &= \boldsymbol{\xi} \cdot \left(\Pi_{n+1} - \Pi_n - \Delta t \int_{\Omega_0} \rho_0 \mathbf{v}_{n+1/2} \times \mathbf{v}_{n+1/2} \right) \\ &= \boldsymbol{\xi} \cdot (\Pi_{n+1} - \Pi_n). \end{aligned} \quad (17)$$

To derive (17), we have used the identity $\hat{\boldsymbol{\xi}} : \boldsymbol{\sigma}_{n+1/2} = 0$ (by definition, $\hat{\boldsymbol{\xi}}$ is skew-symmetric and $\boldsymbol{\sigma}_{n+1/2}$ is symmetric), and the trivial fact $\mathbf{w} \times \mathbf{w} = \mathbf{0}$, $\forall \mathbf{w} \in \mathbb{R}^3$. Due to the arbitrariness of $\boldsymbol{\xi}$, equation (17) is a statement of conservation of angular momentum between time steps n and $n+1$.

3.2. General case: Predictor/multi-corrector

In the predictor/multi-corrector in [1, 2, 7–9], (i) and (j) are finite, and the displacements are updated only after the momentum equation is computed. It is then natural to set $(j) = (i)$ in (14), when attempting to derive a statement of total angular momentum conservation. Hence (14) reduces to

$$0 = \boldsymbol{\xi} \cdot \left(\int_{\Omega_0} \boldsymbol{\varphi}_{n+1/2}^{(i)} \times \rho_0 (\mathbf{v}_{n+1}^{(i+1)} - \mathbf{v}_n) \right) + \Delta t \hat{\boldsymbol{\xi}} : \left(\int_{\Omega_0} \mathbf{F}_{n+1/2}^{(i)} \mathbf{S}_{n+1/2}^{(i)} \mathbf{F}_{n+1/2}^{(i)T} \right). \quad (18)$$

By definition, $\hat{\boldsymbol{\xi}}$ is skew-symmetric, so that, by (11), the second integral in (18) vanishes. This time however, we cannot obtain a straightforward conservation statement for an algorithmic angular momentum defined as

$$\Pi_n^{(i)} := \int_{\Omega_0} \boldsymbol{\varphi}_n^{(i)} \times \rho_0 \mathbf{v}_n^{(i)}. \quad (19)$$

In fact, (18) reduces to

$$\begin{aligned} 0 &= \boldsymbol{\xi} \cdot \int_{\Omega_0} \left(\boldsymbol{\varphi}_n + \frac{\Delta t}{2} \mathbf{v}_{n+1/2}^{(i)} \right) \times \rho_0 (\mathbf{v}_{n+1}^{(i+1)} - \mathbf{v}_n) \\ &= \boldsymbol{\xi} \cdot \left(\int_{\Omega_0} \left(\left(\boldsymbol{\varphi}_n + \frac{\Delta t}{2} \mathbf{v}_{n+1/2}^{(i)} \right) \times (\rho_0 \mathbf{v}_{n+1}^{(i+1)}) \right) - \Pi_n \right) \\ &\quad - \frac{\Delta t}{2} \boldsymbol{\xi} \cdot \left(\int_{\Omega_0} \mathbf{v}_{n+1/2}^{(i)} \times (\rho_0 \mathbf{v}_n) \right) \\ &= \boldsymbol{\xi} \cdot \left(\int_{\Omega_0} \left(\left(\boldsymbol{\varphi}_n + \Delta t \mathbf{v}_{n+1/2}^{(i+1)} \right) \times (\rho_0 \mathbf{v}_{n+1}^{(i+1)}) \right) - \Pi_n \right) \\ &\quad - \frac{\Delta t}{2} \boldsymbol{\xi} \cdot \left(\int_{\Omega_0} (\mathbf{v}_{n+1/2}^{(i+1)} - \mathbf{v}_{n+1/2}^{(i)}) \times (\rho_0 \mathbf{v}_{n+1}^{(i+1)}) \right) \\ &\quad - \frac{\Delta t}{2} \boldsymbol{\xi} \cdot \left(\int_{\Omega_0} \mathbf{v}_{n+1/2}^{(i)} \times (\rho_0 \mathbf{v}_n) \right) \\ &\quad - \boldsymbol{\xi} \cdot \left(\frac{\Delta t}{2} \int_{\Omega_0} \mathbf{v}_{n+1/2}^{(i+1)} \times (\rho_0 \mathbf{v}_{n+1}^{(i+1)}) \right). \end{aligned} \quad (20)$$

Proceeding further, we obtain

$$\begin{aligned} 0 &= \boldsymbol{\xi} \cdot (\Pi_{n+1}^{(i+1)} - \Pi_n) \\ &\quad - \boldsymbol{\xi} \cdot \left(\frac{\Delta t}{2} \int_{\Omega_0} (\mathbf{v}_{n+1/2}^{(i+1)} - \mathbf{v}_{n+1/2}^{(i)}) \times (\rho_0 \mathbf{v}_{n+1}^{(i+1)}) \right) \\ &\quad - \boldsymbol{\xi} \cdot \left(\frac{\Delta t}{2} \int_{\Omega_0} \mathbf{v}_{n+1/2}^{(i)} \times (\rho_0 \mathbf{v}_n) \right) \\ &\quad - \boldsymbol{\xi} \cdot \left(\frac{\Delta t}{2} \int_{\Omega_0} \mathbf{v}_{n+1/2}^{(i+1)} \times (\rho_0 \mathbf{v}_{n+1}^{(i+1)}) \right) \\ &= \boldsymbol{\xi} \cdot (\Pi_{n+1}^{(i+1)} - \Pi_n) \\ &\quad - \boldsymbol{\xi} \cdot \left(\frac{\Delta t}{2} \int_{\Omega_0} (\mathbf{v}_{n+1/2}^{(i+1)} - \mathbf{v}_{n+1/2}^{(i)}) \times (\rho_0 \mathbf{v}_{n+1}^{(i+1)}) \right) \\ &\quad + \boldsymbol{\xi} \cdot \left(\frac{\Delta t}{2} \int_{\Omega_0} (\mathbf{v}_{n+1/2}^{(i+1)} - \mathbf{v}_{n+1/2}^{(i)}) \times (\rho_0 \mathbf{v}_n) \right) \\ &\quad - \boldsymbol{\xi} \cdot \left(\frac{\Delta t}{2} \int_{\Omega_0} \mathbf{v}_{n+1/2}^{(i+1)} \times (\rho_0 (\mathbf{v}_{n+1}^{(i+1)} + \mathbf{v}_n)) \right) \\ &= \boldsymbol{\xi} \cdot (\Pi_{n+1}^{(i+1)} - \Pi_n) \\ &\quad - \boldsymbol{\xi} \cdot \left(\frac{\Delta t}{2} \int_{\Omega_0} \rho_0 (\mathbf{v}_{n+1/2}^{(i+1)} - \mathbf{v}_{n+1/2}^{(i)}) \times (\mathbf{v}_{n+1}^{(i+1)} - \mathbf{v}_n) \right) \\ &\quad - \boldsymbol{\xi} \cdot \left(\Delta t \int_{\Omega_0} \rho_0 \mathbf{v}_{n+1/2}^{(i+1)} \times \mathbf{v}_{n+1/2}^{(i+1)} \right) \\ &= \boldsymbol{\xi} \cdot (\Pi_{n+1}^{(i+1)} - \Pi_n) \\ &\quad - \boldsymbol{\xi} \cdot \left(\frac{\Delta t}{4} \int_{\Omega_0} \rho_0 (\mathbf{v}_{n+1}^{(i+1)} - \mathbf{v}_{n+1}^{(i)}) \times (\mathbf{v}_{n+1}^{(i+1)} - \mathbf{v}_n) \right). \end{aligned} \quad (21)$$

Because $\mathbf{v}_{n+1}^{(i+1)} \neq \mathbf{v}_{n+1}^{(i)}$, this expression shows that $\Pi_{n+1}^{(i+1)} \neq \Pi_n$.

Remark1. As the iterative process proceeds, the error on angular momentum conservation is driven to zero, since

$$\lim_{i \rightarrow \infty} (\mathbf{v}_{n+1}^{(i+1)} - \mathbf{v}_{n+1}^{(i)}) = \mathbf{0}. \quad (22)$$

Using the truncation analysis developed in [5] for the dissipation and phase error, it is possible to give an estimate to the error on total angular momentum conservation, at least in the case of smooth solutions. Proceeding as in [5], Taylor expansions of the dissipation and phase errors for iterate (i) and $(i) \rightarrow \infty$ differ by a term $O(\Delta t^{2i})$. Then

$$\Pi_{n+1}^{(i)} - \Pi_n = \Pi_{n+1}^{(i)} - \Pi_{n+1}^{(\infty)} = O(\Delta t^{2i}), \quad (23)$$

which implies that the global angular momentum conservation error is $O(\Delta t^2)$ for the first iterate, $O(\Delta t^4)$ for the second iterate, $O(\Delta t^6)$ for the third iterate, etc.

It is also possible to derive an expression for an incremental angular momentum quantity that is conserved at each iterate, by casting equation (18) as

$$\int_{\Omega_0} \boldsymbol{\varphi}_{n+1/2}^{(i)} \times \rho_0 (\mathbf{v}_{n+1}^{(i+1)} - \mathbf{v}_n) = \mathbf{0}. \quad (24)$$

Hence, the quantity defined as

$$\hat{\Pi}_{n+1}^{(i+1)} := \Pi_0 + \sum_{k=0}^n \left(\int_{\Omega_0} \boldsymbol{\varphi}_{k+1/2}^{(i)} \times \rho_0 (\mathbf{v}_{k+1}^{(i+1)} - \mathbf{v}_k) \right), \quad (25)$$

where

$$\Pi_0 := \int_{\Omega_0} \boldsymbol{\varphi}_0 \times \rho_0 \mathbf{v}_0, \quad (26)$$

is an exactly conserved quantity. Unfortunately, (25) is not a straightforward definition of total angular momentum.

Remark2. Note that if the choice $(j) = (i+1)$ is made in (13), we would not have obtained a conservation statement either. In fact, algebraic manipulations similar to (17) lead to

$$0 = \boldsymbol{\xi} \cdot (\Pi_{n+1}^{(i+1)} - \Pi_n) + \Delta t \hat{\boldsymbol{\xi}} : \left(\int_{\Omega_0} \mathbf{F}_{n+1/2}^{(i)} \mathbf{S}_{n+1/2}^{(i)} \mathbf{F}_{n+1/2}^{(i+1)T} \right). \quad (27)$$

Due to the iterate mismatch, $\mathbf{F}_{n+1/2}^{(i)} \mathbf{S}_{n+1/2}^{(i)} \mathbf{F}_{n+1/2}^{(i+1)T}$ is not symmetric, and so

$$\Pi_{n+1}^{(i+1)} - \Pi_n \neq 0. \quad (28)$$

Remark3. In numerical computations, mass lumping is most commonly adopted, and the precise definition of the total angular momentum is similar, but not identical to (19), namely

$$\Pi_n^{(i)} := \sum_{A=1}^{n_{np}} \mathbf{x}_{n;A}^{(i)} \times (\mathbf{M}_{0;A} \mathbf{v}_{n;A}^{(i)}), \quad (29)$$

where A is the global node numbering, n_{np} is the total number of nodes in the mesh, \mathbf{x} and \mathbf{v} are the nodal degrees-of-freedom

vectors associated to the position \mathbf{x} and velocity \mathbf{v} , respectively, and

$$\mathbf{M}_{0;A} = \int_{\Omega_0} N_A \rho_0 \, d\Omega_0. \quad (30)$$

It is easy to observe that all previous conclusions apply also in the case of lumped mass matrices, once the algorithmic definition of global angular momentum (29) is substituted in place of (19).

4. Incremental Objectivity

Incremental objectivity is the property for which the action of a stress constitutive model is unchanged under a pure rigid body rotation. In particular, any well posed constitutive model should not produce a change in internal energy, if the motion is given by pure rotation, as a consequence of the fundamental invariance principles in mechanics. This concept can be reformulated [4, 10] in the context of numerical time integration algorithms by evaluating whether objectivity is preserved at the incremental level, between time step n and $n+1$. Consider again the momentum equation (12) with homogeneous Neumann boundary conditions. It is then possible to choose as an admissible variation $\delta \boldsymbol{\varphi} = \frac{1}{2} (\mathbf{v}_{n+1}^{(i+1)} + \mathbf{v}_n)$, to obtain:

$$0 = \frac{1}{2} \int_{\Omega_0} (\mathbf{v}_{n+1}^{(i+1)} + \mathbf{v}_n) \cdot \rho_0 (\mathbf{v}_{n+1}^{(i+1)} - \mathbf{v}_n) + \frac{\Delta t}{2} \int_{\Omega_0} \nabla_x (\mathbf{v}_{n+1}^{(i+1)} + \mathbf{v}_n) : (\mathbf{F}_{n+1/2}^{(i)} \mathbf{S}_{n+1/2}^{(i)}). \quad (31)$$

This easily simplifies to

$$\mathbb{T}_{n+1}^{(i+1)} - \mathbb{T}_n + \frac{\Delta t}{2} \int_{\Omega_0} \nabla_x (\mathbf{v}_{n+1}^{(i+1)} + \mathbf{v}_n) : (\mathbf{F}_{n+1/2}^{(i)} \mathbf{S}_{n+1/2}^{(i)}) = 0, \quad (32)$$

where the total kinetic energy is defined as

$$\mathbb{T}_n^{(i)} := \frac{1}{2} \int_{\Omega_0} \rho_0 \mathbf{v}_n^{(i)} \cdot \mathbf{v}_n^{(i)}. \quad (33)$$

Next, recall that

$$\boldsymbol{\varphi}_{n+1}^{(i+1)} - \boldsymbol{\varphi}_n = \Delta t \mathbf{v}_{n+1/2}^{(i+1)} = \Delta t \frac{\mathbf{v}_{n+1}^{(i+1)} + \mathbf{v}_n}{2}. \quad (34)$$

This can be substituted into equation (32) producing

$$\mathbb{T}_{n+1}^{(i+1)} - \mathbb{T}_n + \int_{\Omega_0} (\mathbf{F}_{n+1}^{(i+1)} - \mathbf{F}_n) : (\mathbf{F}_{n+1/2}^{(i)} \mathbf{S}_{n+1/2}^{(i)}) = 0. \quad (35)$$

This equation represents the change in kinetic energy from the previous time step to the current time step and iterate. In [1, 2, 7–9], to ensure conservation of total energy during the iterative process, the specific internal energy is updated as

$$\begin{aligned} \rho_0 (\mathcal{E}_{n+1}^{(i+1)} - \mathcal{E}_n) &= (\mathbf{F}_{n+1}^{(i+1)} - \mathbf{F}_n) : (\mathbf{F}_{n+1/2}^{(i)} \mathbf{S}_{n+1/2}^{(i)}) \\ &= \mathbf{F}_{n+1/2}^{(i)T} (\mathbf{F}_{n+1}^{(i+1)} - \mathbf{F}_n) : \mathbf{S}_{n+1/2}^{(i)}. \end{aligned} \quad (36)$$

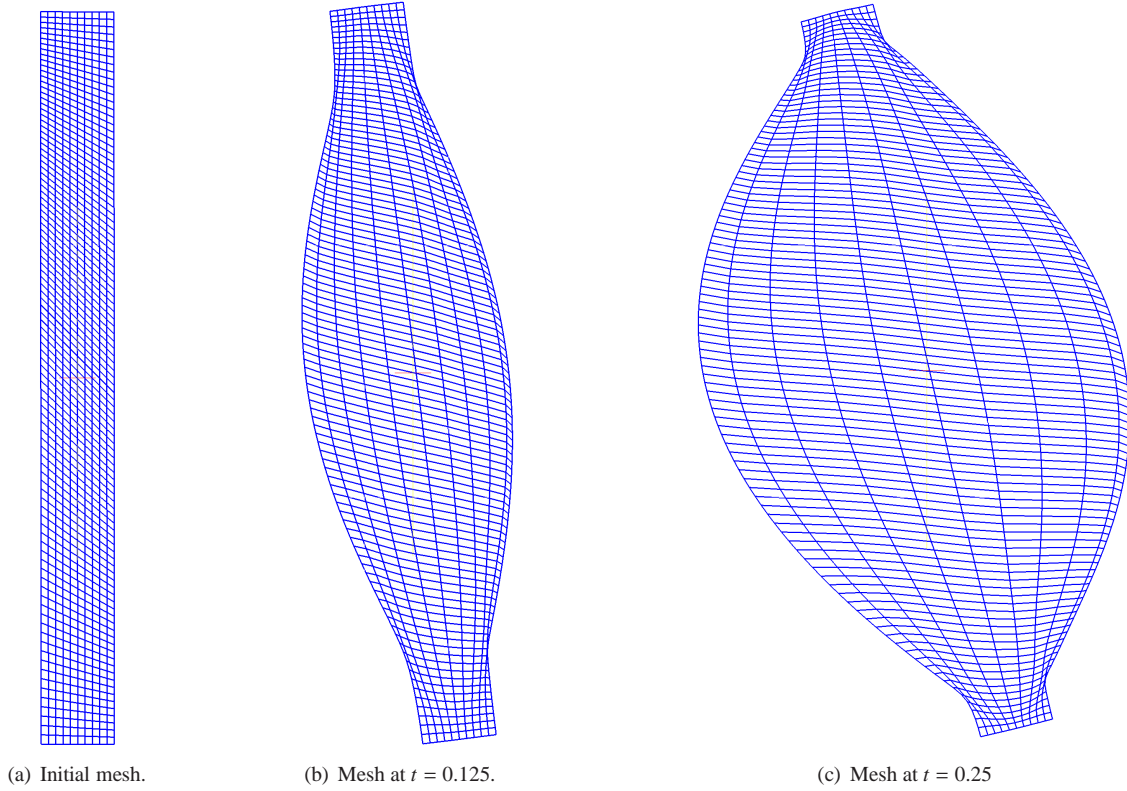


Figure 2: Initial mesh configuration and time evolution of mesh deformation for a numerical test of global angular momentum conservation. The initial velocity is given by a rigid body rotation field. The initial density is unity, the initial energy is given by (46). As the material rotates due to the initial velocity condition, the pressure relaxes and the flow expands.

Noting that

$$\mathbf{F}_{n+1/2}^{(i)} = \frac{1}{2} (\mathbf{F}_{n+1}^{(i)} + \mathbf{F}_n), \quad (37)$$

this can be algebraically expanded to yield

$$\begin{aligned} \rho_0(\varepsilon_{n+1}^{(i+1)} - \varepsilon_n) &= \frac{1}{2} (\mathbf{F}_{n+1}^{(i)T} \mathbf{F}_{n+1}^{(i+1)} - \mathbf{F}_{n+1}^{(i)T} \mathbf{F}_n) : \mathbf{S}_{n+1/2}^{(i)} \\ &+ \frac{1}{2} (\mathbf{F}_n^T \mathbf{F}_{n+1}^{(i+1)} - \mathbf{F}_n^T \mathbf{F}_n) : \mathbf{S}_{n+1/2}^{(i)}. \end{aligned} \quad (38)$$

Consider initially the limit case as $(i) \rightarrow \infty$ and the fixed-point iteration converges. Then,

$$\begin{aligned} \rho_0(\varepsilon_{n+1} - \varepsilon_n) &= \frac{1}{2} (\mathbf{F}_{n+1}^T \mathbf{F}_{n+1} - \mathbf{F}_n^T \mathbf{F}_n) : \mathbf{S}_{n+1/2} \\ &+ \frac{1}{2} (\mathbf{F}_n^T \mathbf{F}_{n+1} - \mathbf{F}_{n+1}^T \mathbf{F}_n) : \mathbf{S}_{n+1/2}. \end{aligned} \quad (39)$$

Recalling that \mathbf{S} is symmetric, that $\mathbf{F}_n^T \mathbf{F}_{n+1} - \mathbf{F}_{n+1}^T \mathbf{F}_n$ is skew-symmetric, and that $\mathbf{C} = \mathbf{F}^T \mathbf{F}$, this simplifies to

$$\rho_0(\varepsilon_{n+1} - \varepsilon_n) = \frac{1}{2} (\mathbf{C}_{n+1} - \mathbf{C}_n) : \mathbf{S}_{n+1/2}. \quad (40)$$

Assume that the incremental motion over the time step Δt is a rigid rotation. Then $\mathbf{F}_{n+1} = \mathbf{Q} \mathbf{F}_n$ for some $\mathbf{Q} \in SO(3)$ (the group of proper orthogonal rotations). This implies that $\mathbf{C}_{n+1} = \mathbf{C}_n$ and thus $\varepsilon_{n+1} = \varepsilon_n$. Now consider the non-limit case where

$(i) < \infty$ and the fixed-point iteration is not converged. Hence,

$$\begin{aligned} \rho_0(\varepsilon_{n+1}^{(i+1)} - \varepsilon_n) &= \frac{1}{2} (\mathbf{F}_{n+1}^{(i)T} \mathbf{F}_{n+1}^{(i+1)} - \mathbf{C}_n) : \mathbf{S}_{n+1/2}^{(i)} \\ &+ \frac{1}{2} (\mathbf{F}_n^T \mathbf{F}_{n+1}^{(i+1)} - \mathbf{F}_{n+1}^{(i)T} \mathbf{F}_n) : \mathbf{S}_{n+1/2}^{(i)}. \end{aligned} \quad (41)$$

Observe that

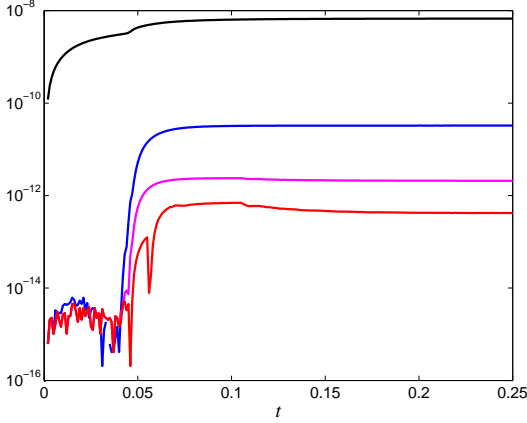
$$\mathbf{F}_{n+1}^{(i)T} \mathbf{F}_{n+1}^{(i+1)} \neq \mathbf{C}_{n+1}^{(i+1)} \quad (42)$$

and that $\mathbf{F}_n^T \mathbf{F}_{n+1}^{(i+1)} - \mathbf{F}_{n+1}^{(i)T} \mathbf{F}_n$ is not a skew tensor in general. Therefore, equation (41) cannot easily be simplified any further due to the ‘‘mismatching’’ terms involving (i) and $(i+1)$.

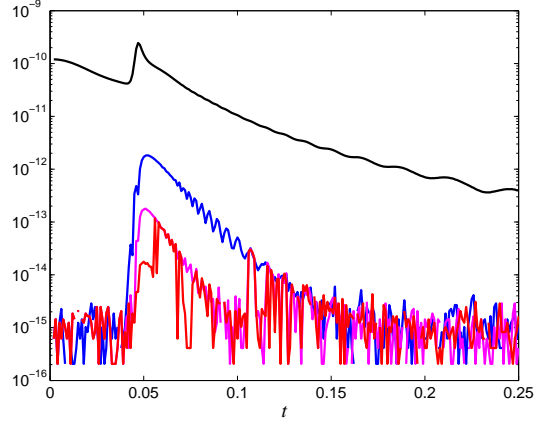
Remark4. The predictor-corrector algorithm is incrementally objective if the fixed-point iteration is driven to convergence. Derivations analogous to the ones leading to (23) allow estimation of the order of accuracy with which incremental objectivity is approximated. In fact, using the Taylor expansion results in [5], we obtain

$$\varepsilon_{n+1}^{(i)} - \varepsilon_n = \varepsilon_{n+1}^{(i)} - \varepsilon_{n+1}^{(\infty)} = O(\Delta t^{2i}). \quad (43)$$

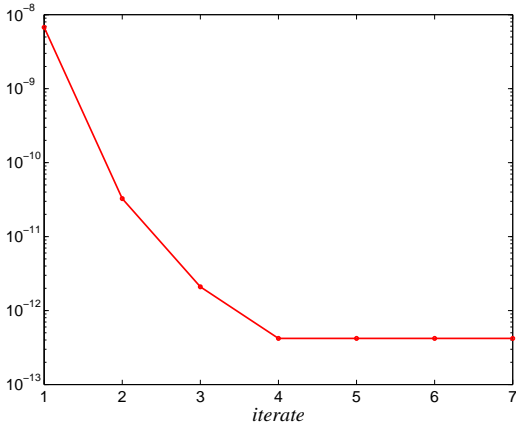
Remark5. It is also important to notice that exact incremental objectivity is an important requirement in constitutive modeling for solid mechanics applications, while it is usually considered less critical in fluid mechanics computations. In fact, it is very frequent and widespread in computational fluid mechanics to use non-objective time integration algorithms [3].



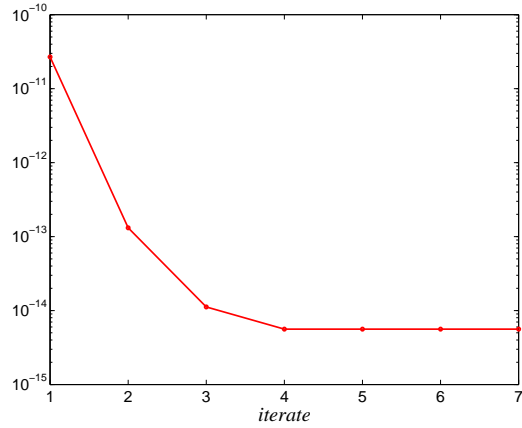
(a) $\Delta\Pi(t)$, various iterates.



(b) $\Delta_n\Pi$, various iterates.



(c) Semi-logarithmic plot, $\Delta\Pi(t = 0.25)$.



(d) Semi-logarithmic plot, $\langle\Delta_n\Pi\rangle_N$.

Figure 3: Evolution of global angular momentum for the problem specified by (44)–(46). Figure 3(a) shows the time history of the relative error in global angular momentum $\Delta\Pi(t)$, for various iterates of the predictor/multi-corrector. Figure 3(b) shows the time history of the relative increment of global angular momentum $\Delta_n\Pi$. In Figures 3(a) and 3(b) the black, blue, magenta, and red lines indicate the first, second, third, and fourth iterates, respectively. Figure 3(c) shows a semi-logarithmic plot of $\Delta\Pi(t = 0.25)$ as a function of the number of iterates of the predictor/multi-corrector. Figure 3(d) shows a semi-logarithmic plot of the average relative increment of angular momentum $\langle\Delta_n\Pi\rangle_N$, as a function of the number of iterates of the predictor/multi-corrector.

5. A numerical experiment

In order to verify the previous statements, we have designed a simple experiment. Let us consider the rectangular domain $[-0.5, 0.5] \times [-0.05, 0.05]$, with superposed the mesh shown in Figure 2(a) (commonly referred to as the Saltzman mesh, see [6, 8, 9], and references therein, for more details). The material is an ideal gas with $\gamma = 5/3$, for which $\sigma = -p\mathbf{I}_{n_d \times n_d}$, with $p = (\gamma - 1)\rho\epsilon$. Consider also the following initial conditions for the velocity, density, and internal energy:

$$\mathbf{v}_0 = [-x_2, x_1], \quad (44)$$

$$\rho_0 = 1.0, \quad (45)$$

$$\epsilon_0 = \frac{1 - \cos(2\pi(x + 0.5))}{4} \times \left(1 - \cos\left(\frac{2\pi}{0.1}(y + 0.05)\right) \right). \quad (46)$$

Hence the initial velocity field represents a rigid body rotation around the origin, while the internal energy has a cosine profile along both the x_1 and x_2 directions, and vanishes at the boundary of the domain. Zero-traction boundary conditions are applied on the entire boundary (homogeneous Neumann boundary conditions). As seen in Figures 2(b) and 2(c), the flow rotates, due to the initial condition on the velocity, and at the same time it expands, as the initial distribution of pressure relaxes toward equilibrium ($p = 0$). Given the specifications of the initial/boundary value problem, global angular momentum is conserved.

Figure 3 shows the time history of the following quantities: The relative error in global angular momentum (with respect to the initial condition)

$$\Delta\Pi(t) = \frac{\Pi(t) - \Pi_0}{\Pi_0} = \frac{\Pi(t)}{\Pi_0} - 1, \quad (47)$$

the relative increment in global angular momentum

$$\Delta_n \Pi = \frac{\Pi_{n+1} - \Pi_n}{\Pi_n} = \frac{\Pi_{n+1}}{\Pi_n} - 1, \quad (48)$$

and the average relative increment in global angular momentum

$$\langle \Delta_n \Pi \rangle_N = \frac{1}{N} \sum_{n=0}^{N-1} \Delta_n \Pi. \quad (49)$$

Because the flow solution is smooth, it is easy to appreciate the rapid decay of the various measures of global angular momentum, as the number of iterations increases. As seen in Figures 3(c) and 3(d), the error in global angular momentum is within machine precision for 4 or more iterates.

6. Summary

We have presented an analysis aimed at evaluating the total angular momentum conservation and incremental objectivity properties of algorithms in the predictor/multi-corrector class documented in [1, 2, 7–9]. When convergence of the iterative algorithm is attained, total angular momentum is conserved exactly, and incremental objectivity is satisfied exactly. This is not the case for a finite iterate ($i + 1$) of the predictor/multi-corrector procedure, and the numerical approximation error has been estimated to scale as Δt^{2i} , using a Taylor series expansion argument.

Acknowledgments

The authors would like to thank, for very valuable discussions, Professor T. J. R. Hughes at the University of Texas in Austin, Dr. L. Margolin and Dr. M. Shashkov at Los Alamos National Laboratory, and Dr. W. J. Rider at Sandia National Laboratories. The authors would also like to thank Dr. R. Summers and Dr. S. Collis, at Sandia National Laboratories, for support and encouragement during the development of this research work.

References

- [1] A. Barlow. A compatible finite element multi-material ALE hydrodynamics algorithm. *International Journal for Numerical Methods in Fluids*, **56**(8):953–964, 2008.
- [2] E. J. Caramana, M. J. Shashkov, and P. P. Whalen. Formulations of artificial viscosity for multi-dimensional shock wave computations. *Journal of Computational Physics*, **144**:70–97, 1998.
- [3] P. M. Gresho and R. L. Sani. *Incompressible Flow and the Finite Element Method*. Wiley, New York, NY, 2000.
- [4] T. J. R. Hughes and J. Winget. Finite rotation effects in numerical integration of rate constitutive equations arising in large-deformation analysis. *International Journal for Numerical Methods in Engineering*, **15**(12):1862–1867, 1980.
- [5] E. Love, W. J. Rider, and G. Scovazzi. Stability analysis of a predictor/multi-corrector method for staggered-grid Lagrangian shock hydrodynamics. *Journal of Computational Physics*, 2009. Submitted.
- [6] G. Scovazzi, M. A. Christon, T. J. R. Hughes, and J. N. Shadid. Stabilized shock hydrodynamics: I. A Lagrangian method. *Computer Methods in Applied Mechanics and Engineering*, **196**(4–6):923–966, 2007.
- [7] G. Scovazzi, E. Love, and M. J. Shashkov. A multi-scale Q1/P0 approach to Lagrangian shock hydrodynamics. Technical report, SAND2007-1423, Sandia National Laboratories, New Mexico, March 2007. Available at: <http://www.cs.sandia.gov/~gscovaz>.
- [8] G. Scovazzi, E. Love, and M. J. Shashkov. A multi-scale Q1/P0 approach to Lagrangian shock hydrodynamics. *Computer Methods in Applied Mechanics and Engineering*, **197**(9–12):1056–1079, 2008.
- [9] G. Scovazzi, J. N. Shadid, E. Love, and T. J. R. Hughes. Stabilized shock hydrodynamics: IV. Computations with a conservative updated Lagrangian method. *Computer Methods in Applied Mechanics and Engineering*, 2009. Submitted.
- [10] J. C. Simo and T. J. R. Hughes. *Computational Inelasticity*. Springer, New York, 1998.
- [11] J. C. Simo and N. Tarnow. The discrete energy-momentum method. Conserving algorithms for nonlinear elastodynamics. *Zeitschrift für Angewandte Mathematik und Physik (ZAMP)*, **43**(5):757–792, 1992.